



Energy and climate effects of second-life use of electric vehicle batteries in California through 2050



Roger Sathre ^{a,*}, Corinne D. Scown ^a, Olga Kavvada ^{a,b}, Thomas P. Hendrickson ^{a,b}

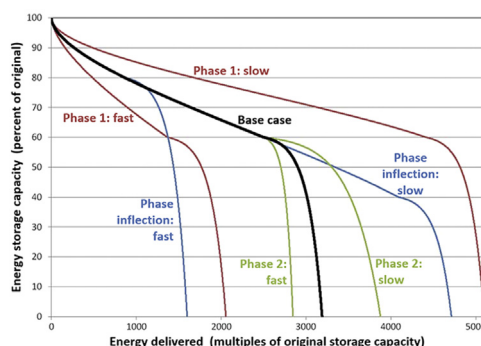
^a Energy Technologies Area, Lawrence Berkeley National Laboratory, Berkeley, CA 94720, USA

^b Department of Civil and Environmental Engineering, University of California, Berkeley, CA 94720, USA

HIGHLIGHTS

- We model potential second-life use of retired PEV batteries for stationary storage.
- Second-life batteries in California may deliver ~15 TWh per year in 2050.
- Enabled renewable electricity generation may displace ~7 Mt CO₂e per year in 2050.
- There is significant uncertainty in PEV adoption and battery degradation scenarios.
- We calculate ESOI and discuss appropriate metrics for large-scale storage systems.

GRAPHICAL ABSTRACT



ARTICLE INFO

Article history:

Received 7 March 2015

Received in revised form

13 April 2015

Accepted 16 April 2015

Available online

Keywords:

Battery

Lithium ion

Degradation

Energy balance

Climate change mitigation

Grid storage

ABSTRACT

As the use of plug-in electric vehicles (PEVs) further increases in the coming decades, a growing stream of batteries will reach the end of their service lives. Here we study the potential of those batteries to be used in second-life applications to enable the expansion of intermittent renewable electricity supply in California through the year 2050. We develop and apply a parametric life-cycle system model integrating battery supply, degradation, logistics, and second-life use. We calculate and compare several metrics of second-life system performance, including cumulative electricity delivered, energy balance, greenhouse gas (GHG) balance, and energy stored on invested. We find that second-life use of retired PEV batteries may play a modest, though not insignificant, role in California's future energy system. The electricity delivered by second-life batteries in 2050 under base-case modeling conditions is 15 TWh per year, about 5% of total current and projected electricity use in California. If used instead of natural gas-fired electricity generation, this electricity would reduce GHG emissions by about 7 million metric tons of CO₂e per year in 2050.

Published by Elsevier B.V.

1. Introduction

The usage of plug-in electric vehicles (PEVs) is increasing rapidly, driven by concerns about environmental quality and energy security. PEV sales in the United States (US) increased by a factor of over 5 between 2011 and 2013, from 18,000 to 100,000

* Corresponding author.

E-mail address: rsathre@lbl.gov (R. Sathre).

vehicles per year [1]. One report projected that PEVs will comprise 30% of US light-duty vehicle sales by 2030, and 80% by 2050 [2]. The state of California leads PEV sales in the US, accounting for almost one-third of total US PEV sales [3]. As these vehicles age, a growing number of PEV batteries will reach the end of their service lives. If the current California vehicle fleet were fully electrified, it would entail a post-use battery flow of about 900,000 metric tons per year [4]. Recycling is typically considered as the default end-of-life management for PEV batteries. However, these batteries may retain as much as 70–80% of their original storage capacity at the point of retirement. Stationary energy storage applications, where storage capacity and power per unit mass are less critical constraints, offer a potentially attractive option for extending PEV batteries' useful life [5]. Referred to as second-life, using post-consumer PEV batteries as grid-connected stationary energy storage comes with economic, energetic, and environmental tradeoffs. Quantitatively assessing these tradeoffs and the relative scale of second-life batteries' contribution to overall energy storage goals may inform future research and policy decisions.

Previous research has explored various aspects of second-life PEV battery use, with a focus on economic viability. In a pioneering study, Cready et al. [6] considered the techno-economic potential of using retired PEV batteries for a range of second-life applications, identifying 4 promising candidates: transmission support, light commercial load following, residential load following, and distributed node telecommunications backup power. They observed that major uncertainties exist regarding the performance and life span of used PEV batteries. Narula et al. [7] conducted an economic analysis of PEV batteries used for various second-life applications, assuming a fixed (either 5- or 10-year) service life. They found marginal economic benefits for single-use applications, although results improved with multiple simultaneous applications, e.g. area regulation, transmission and distribution upgrade deferral, and energy time shifting. Neubauer & Pesaran [8] assessed the economic impact that second-life batteries use may have on initial PEV costs. They found the upfront cost reductions to be relatively minor, and strongly dependent on the battery degradation profile and specific second-life application. Williams & Lipman [9] analyzed the potential economic impacts of second-life battery use, finding modest but positive economic benefits of second-life battery use. Benefits depended largely on whether multiple services could be obtained from the batteries, and on costs associated with power-conditioning equipment. Neubauer et al. [10] estimated the selling price of re-purposed PEV batteries, and found them to be cost-competitive with established lead-acid battery technology. Ambrose et al. [11] considered the potential for retired PEV batteries to provide electricity storage for rural micro-grids in developing regions, concluding that second-life lithium-ion batteries may be price competitive with new lead-acid batteries and deliver improved performance.

Fewer studies have considered the environmental or energetic implications of second-life battery use. Ahmadi et al. [12] estimated the potential CO₂ emissions reduction of using repurposed vehicle batteries to store off-peak electricity in Canada, thus avoiding natural gas-fired peak generation. Faria et al. [13] conducted an environmental assessment of second-life PEV battery use for peak shaving and load shifting, based on grid characteristics of several European countries. Both studies found that greenhouse gas (GHG) emissions reduction from second-life use depends strongly on the carbon-intensity of the electricity sources involved, but neither explored the sensitivity of the results to highly uncertain system parameters including battery degradation and capacity thresholds of first- and second-life use.

PEV adoption and the availability of retired batteries will grow alongside an evolving energy supply system, including increasing

amounts of renewable electricity sources. The intermittency of these sources, such as solar and wind, requires energy storage for maximum performance. In this study, we explore the extent to which second-life use of retired PEV batteries can provide this electricity storage role. We seek to address several research questions in this analysis. First, we determine which factors most significantly affect the net-energy balance of second-life battery usage. Second, we quantify the potential contribution of second-life batteries to California's energy storage needs through 2050. Last, we quantify the net life-cycle GHG benefits from using second-life batteries to support intermittent renewable electricity sources.

2. Methods

2.1. Modeling framework

We develop and apply a parametric life cycle model to describe the interrelated energy and material flows of the PEV battery system. The model is driven by scenarios of future adoption of PEVs in California, and the resulting stream of retired PEV batteries. We focus on the potential for second-life usage of the retired batteries and its net impact on energy use and greenhouse gas (GHG) emissions, while assuming other life-cycle phases (battery manufacture, first life, and final recycling) remain unchanged. The system boundaries of this study include all direct impacts of second-life use such as battery transport, thermal management, and charging. The boundaries also encompass components of the broader energy system, including the displacement of fossil energy production by enabling diurnal energy shifting of intermittent renewable electricity production. The analytical framework is shown schematically in Fig. 1. We assume that future electricity output from renewable sources will exceed demand during peak generation times, and electricity storage allows the use of this electricity later in the diurnal cycle during peak demand times.

Based on modeled material and energy flows through the year 2050, we calculate and compare several metrics of second-life system performance. These include the electricity delivered, the energy balance, the GHG balance, and the energy stored on invested. The electricity delivered is simply the summation of the electrical energy discharged from the second-life batteries, in units of TWh. This can be expressed on an annual basis, or cumulative over the study period (2015–2050).

The energy balance is a summation of major energy flows throughout the system, and is defined by Equation (1):

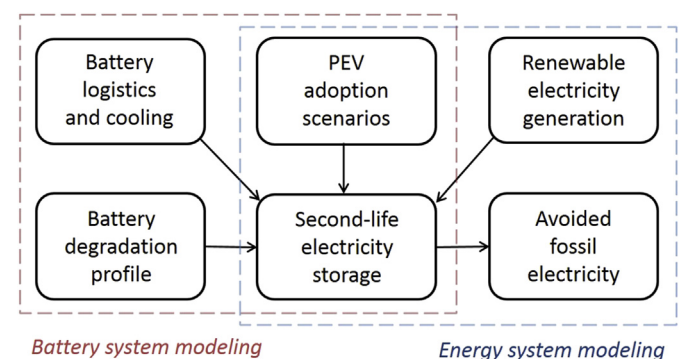


Fig. 1. Schematic diagram of analytical framework integrating battery system modeling with broader energy system modeling. Electricity storage in second-life PEV batteries enables dispatchable output of intermittent renewable electricity, thus avoiding fossil electricity generation. Scenario modeling of PEV adoption and battery degradation defines the scale of the operation.

$$\text{Energy Balance} = E_{\text{delivered}} - E_{\text{charging}} - E_{\text{cooling}} - E_{\text{transport}} \quad (1)$$

where $E_{\text{delivered}}$ is the electrical energy delivered by the batteries during their second life, E_{charging} is the electrical energy used to charge the batteries during their second life, E_{cooling} is the electrical energy used for cooling of batteries during their second life, and $E_{\text{transport}}$ is the energy used to transport batteries to and from their second-life applications. Equation (1) is based on the assumption that, for the sites considered in this analysis, the thermal management system must only provide cooling. Yuksel & Michalek [14] show that battery performance decreases at temperatures both higher and lower than the optimum of 15–20 °C. Typical high temperatures in most of California are more likely to be problematic than lows, though the opposite is true for states with colder climates such as Minnesota. We account for energy in units of TWh of electrical energy, or its equivalent. We assume energy used for battery transport is diesel fuel for trucks, thus we divide the TWh of diesel used by a factor of 3, corresponding to an assumed conversion efficiency of 33% from diesel fuel to equivalent electricity. Energy balance can be calculated and expressed per year on an annual basis, and can also be cumulated and expressed through the year 2050.

The cumulative GHG balance is a summation of actual and avoided GHG emissions to the atmosphere through 2050, and is defined by Equation (2):

$$\text{GHG Balance} = \text{GHG}_{\text{charging}} + \text{GHG}_{\text{cooling}} + \text{GHG}_{\text{transport}} - \text{GHG}_{\text{avoided}} \quad (2)$$

where $\text{GHG}_{\text{charging}}$ is the cumulative GHG emissions from producing electricity to charge the batteries during their second life, $\text{GHG}_{\text{cooling}}$ is the cumulative GHG emissions from producing electricity to cool the batteries during their second life, $\text{GHG}_{\text{transport}}$ is the GHG emissions from transporting the batteries to and from their second-life applications, and $\text{GHG}_{\text{avoided}}$ is the cumulative GHG emissions avoided by not generating fossil-based electricity during peak demand times. We account for GHG emissions in units of million metric tons of CO₂ equivalent (Mt CO₂e). The GHG balance can be expressed on both annual and cumulative bases.

Energy stored on energy invested (ESOI) was introduced by Barnhart & Benson [15] to compare the energy stored and delivered by a device during its service life, to the energy needed to manufacture the device. Barnhart & Benson [15] defined ESOI with Equation (3):

$$\text{ESOI}_{B\&B} = \frac{C_0 \times \lambda \times \eta \times D}{C_0 \times \varepsilon} \quad (3)$$

where C_0 is the initial storage capacity of the battery, λ is the number of cycles in the battery's service life, η is the round-trip charge–discharge efficiency, D is the depth of discharge, and ε is the cradle-to-gate embodied primary energy per unit of electrical storage capacity. This definition is of limited use for battery second-life analysis, as it does not explicitly consider battery degradation during the service life, the numerator (“energy stored”) does not distinguish between energy stored during first and second lives, and the denominator (“energy invested”) includes only the energy used at the beginning of the life cycle for material sourcing and battery manufacturing. We note also that round-trip losses are accounted for in the numerator as a reduction of the energy stored, rather than in the denominator as a component of operational energy investment.

Here we require a metric that distinguishes between energy stored during first and second lives, as well as between energy

inputs during manufacturing, operation, reconfiguration, and end-of-life stages. We adapt the ESOI metric by considering in the numerator only the energy stored and delivered during the second life, and in the denominator the direct transport and cooling energy inputs needed to enable this second life. We define ESOI' with Equation (4):

$$\text{ESOI}' = \frac{E_{\text{delivered}}}{E_{\text{cooling}} + E_{\text{transport}}} \quad (4)$$

where $E_{\text{delivered}}$, E_{cooling} and $E_{\text{transport}}$ are as defined in Equation (1). Further seeking to refine the metric, we then define ESOI'' that also includes round-trip efficiency losses in the denominator (Equation (5)).

$$\text{ESOI}'' = \frac{E_{\text{delivered}}}{E_{\text{transport}} + E_{\text{cooling}} + E_{\text{loss}}} \quad (5)$$

where E_{loss} is defined in Equation (6):

$$E_{\text{loss}} = E_{\text{delivered}} \left(\frac{1}{\eta} - 1 \right) \quad (6)$$

where η is the round-trip charge–discharge efficiency. The ESOI'' metric (Equation (5)) considers the round-trip efficiency loss as invested operational energy input, rather than as reduction of delivered energy as in Barnhart & Benson's definition (Equation (3)). We observe that a comprehensive full life-cycle ESOI metric for batteries would include in the numerator all the electricity delivered during first- and second-life operation, and in the denominator all the energy used for material sourcing, manufacture, operation, reconfiguration and disposal.

The system model consists of four elements: Battery supply, battery degradation, battery second-life use, and battery logistics. These are described in the following sections.

2.2. Battery supply

A crucial input for our analysis is the total quantity of batteries made available for second-life applications each year, which is largely determined by future PEV market adoption rates. Our scenarios are based on well-established fleet modeling equations. We use a sigmoid adoption curve, documented by Scown et al. [16], to represent the growing market share of PEVs (Equation (7)):

$$P(t) = \frac{1}{1.41(1 + e^{-0.25t+5})} \quad (7)$$

where $P(t)$ is the base-case PEV penetration (fraction) of total US automobile sales, and t is the years elapsed since 2015. We consider a base-case adoption rate, as well as low and high variations to assess uncertainty. The base-case scenario reaches a 70% PEV share of passenger car sales by 2050, while the low growth scenario reaches approximately 60% and the high growth scenario reaches approximately 80%. Baseline vehicle sales are provided by the US Energy Information Administration [17], which we use to track each vehicle in the fleet from sale to retirement, beginning with cars sold in the 1970s. California's total car sales are allocated to counties based on population. The bases for our assumptions are documented in Scown et al. [16].

PEVs' share of sales growth in each county is modeled using several factors. “Early adopter” urban counties including Los Angeles, San Francisco, and Alameda, for example, are responsible for the bulk of the early growth, which is consistent with preliminary sales data. These urban areas tend to be the first to install

PEV supporting infrastructure such as publicly available charging stations. The remaining groups are categorized based on affluence, quantified as median income (see [Tables S1 and S2](#)). As each new adoption group enters the scenario, sales growth is allocated to individual counties based on population. Results of these scenarios by county for 2020, 2030, 2040 and 2050 are shown in [Fig. S1](#).

We then translate PEV market adoption scenarios into battery disposal estimates. We use logistic curves to represent the fraction of batteries remaining after a given number of years beyond its initial purchase date. In the base-case scenario, 75% of batteries last 10 years or longer. We also consider a short duration scenario where only 60% of batteries last 10 years or longer, and a long duration scenario where 90% of batteries last 10 years or longer. Cars may, however, outlast their batteries, so we assume that new batteries are purchased for cars that remain in use, but whose batteries have reached their end-of-life. However, we assume that cars within 2 years of their end-of-life will be retired early rather than have a new battery installed. We estimate the fraction of vehicles remaining on the road (FVR) using Equation (8) [18]:

$$FVR(a) = \frac{1}{1 + e^{-0.28(16.9-a)}} \quad (8)$$

where a is the vehicle age in years.

High and low variations in battery supply for second-life use are determined by combinations of PEV adoption rate scenarios and in-vehicle battery duration scenarios that yield the highest and lowest supply of retired batteries. Additional details of our adoption and disposal scenarios are provided in the Supporting Information, including assumptions about battery capacities ([Figs. S3 and S4](#)) and the R script.

2.3. Battery degradation

It is broadly understood that battery performance degrades with usage and time, but comprehensive and quantitative description of such degradation remains elusive. More is known about early stages of battery degradation, such as the growth of solid electrolyte interface [19]. Less is known about later stages of degradation such as lithium plating, growth of dendrites, and structural failure [20]. This makes the robust modeling of life-cycle battery performance more challenging, as the literature lacks detailed quantitative description of the latter stages of battery life.

It is generally recognized that a battery will experience an initial capacity loss that decreases in rate, after which an inflection point is reached and the battery suffers terminal degradation that increases in rate [21]. In this analysis, we develop a simple model to generically describe this pattern of life-cycle PEV battery degradation based on 3 parameters: Phase 1 initial degradation rate, Phase inflection point, and Phase 2 terminal degradation rate. The energy storage capacity of the battery is tracked over time, expressed as a percent of the capacity when the battery was new. Phase 1 of the degradation profile is described mathematically by Equation (9):

$$C_1 = 100 - (303 \times D^X) \quad (9)$$

where C_1 is the energy storage capacity of the battery during Phase 1 (expressed as percent of original capacity), D is the ideal cumulative energy discharged from the battery (disregarding capacity loss), and X is an exponential factor with a base-case value of 0.55. This equation is based on Wang et al. [22], who considered the ideal cumulative energy discharge (D) as the number of cycles multiplied by the depth of discharge multiplied by the full cell capacity (i.e. not including the effects of capacity degradation). We recalculate the

cumulative energy discharge accounting for battery degradation, and conduct our analysis based on cumulative energy delivered by the battery, expressed in multiples of original storage capacity. The capacity loss function corresponds to graphite-LiFePO₄ cells with a charge/discharge rate of 2C and a temperature of 60 °C (Equation (7) from Reference [22]). We acknowledge that other Li-ion battery chemistries and usage conditions will result in other degradation patterns, though due to the paucity of robust literature data we assume these uncertainties are accommodated within our parameter variations. We vary the Phase 1 degradation rate by changing the value of the exponential factor X from its base-case value of 0.55, to a faster degradation value of 0.60 and a slower degradation value of 0.50.

We model the inflection point between initial Phase 1 and terminal Phase 2 degradation, specified as a percentage of original energy storage capacity. In the absence of more compelling data, we assume a base-case inflection point at 60% of original capacity, with values of 80% and 40% corresponding to faster and slower degradation. We then model the terminal Phase 2 degradation based on exponential decay defined by Equation (10):

$$C_2 = P - 1.006^{(E \times Y)} \quad (10)$$

where C_2 is the energy storage capacity of the battery during Phase 2 (expressed as percent of original capacity), P is the location of the inflection point between Phases 1 and 2 (in percent of original capacity), and E is the cumulative energy delivered by the battery during Phase 2 (in multiples of original full storage capacity), and Y is a multiplier. We vary the Phase 2 degradation rate by changing the value of the multiplier Y from its base case value of 1, to a faster degradation value of 2 and slower degradation value of 0.5. Our base-case degradation profile, as well as profiles representing variations of each parameter, is shown in [Fig. 2](#). The slight discontinuity of some profiles is due to the different slopes of Equation (9) and Equation (10) at the inflection point, and has no fundamental effect on the analysis.

Within each defined battery degradation profile, we consider various arrangements for first and second lives. Our base-case condition assumes the first life (as a PEV battery) continues until the energy storage capacity decreases to a threshold value of 70% of its original value when the car was new. We then assume the battery pack (or its disassembled cells) is placed into a stationary second-life application, which continues until the storage capacity declines to a final threshold, assumed to be 30% in our base case. This is illustrated in [Fig. 3](#) for the base-case conditions, where 53% of total life-cycle electricity is delivered during the first-life and 47% is delivered during the second-life. [Fig. S2](#) shows corresponding results for alternative values of battery degradation parameters. To determine the significance of different threshold locations, we vary the first-life threshold between 60% and 80%, and the second-life threshold between 20% and 40%.

2.4. Battery second-life use

We consider the use of second-life PEV batteries to enable diurnal energy shifting, allowing expanded use of intermittent renewable energy sources such as wind and solar. We assume that this daily storage and discharge of renewable electricity will substitute electricity generation from natural gas-fired power plants. In a sensitivity analysis we consider the substitution of electricity from coal-fired power plants. Although coal-fired electricity is unlikely in California, the second-life batteries may, in principle, be used in other locations where coal-fired power is more common. Our base-case analysis assumes second-life batteries are used in decentralized photovoltaic (PV) facilities, while we consider

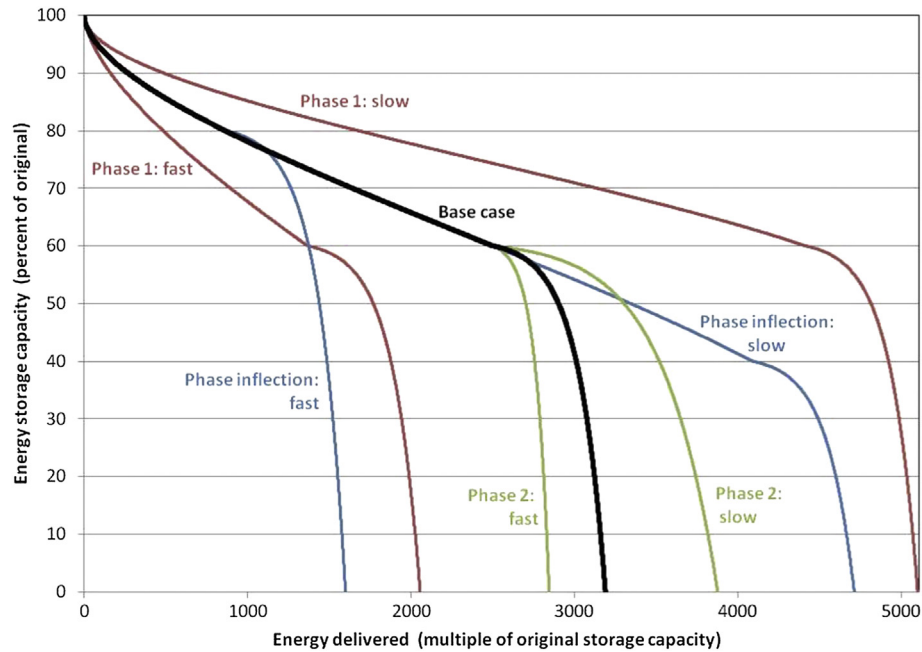


Fig. 2. Modeled range of battery degradation profiles, each composed of an initial Phase 1 degradation, followed by a Phase inflection point and terminal Phase 2 degradation. Each of these parameters is defined by a base case value, as well as by values describing faster or slower degradation.

decentralized wind and centralized renewable generation in a sensitivity analysis (see Section 2.5). GHG emission intensity factors for electricity generation are based on median values from recent life-cycle assessment (LCA) harmonized meta-analyses. For wind electricity, 15 gCO₂e are emitted per kWh, based on Dolan & Heath [23]. For PV electricity, 27 gCO₂e are emitted per kWh, based on average emission factors for crystalline silicon PV [24] and thin-film PV [25]. Emission factors for natural gas-fired electricity are 510 gCO₂e per kWh based on O'Donoghue et al. [26], while those for coal-fired electricity are 980 gCO₂e per kWh based on Whitaker et al. [27]; both are average values for a range of energy conversion technologies. We assume the use of an integrated battery management system, to avoid capacity imbalance when cells of different degradation levels are assembled together [28,29].

We consider the direct energy use and GHG emissions from activities needed to enable second-life applications, including

battery cooling. Cooling of batteries during use is important to avoid premature degradation and temporary efficiency losses, particularly in California and other warm climates. A recent study shows that an ambient temperature of 32 °C can reduce a Nissan Leaf battery pack's round-trip charge/discharge efficiency by greater than 20% relative to optimal conditions (15–20 °C), and an ambient temperature of 38 °C can reduce efficiency by more than 30% [14]. We quantified the waste heat to be removed based on the round trip efficiency of the batteries, and the cooling energy inputs based on the coefficient of performance (COP) of the cooling system. This is described by Equation (11):

$$E_{cooling} = E_{delivered} \times \frac{1 - \eta}{COP} \quad (11)$$

where $E_{cooling}$ is the electrical energy needed for battery cooling, $E_{delivered}$ is the electricity delivered by the batteries, η is the round-trip charge/discharge efficiency of the batteries, and COP is the coefficient of performance of the cooling system (ratio of heat removed to electrical energy input). Our base-case analysis assumes a round-trip efficiency of 80% for the second-life batteries, and a COP of 4. In a sensitivity analysis, we consider a round-trip efficiency range of 70%–90%, and a COP range of 2–6.

2.5. Battery logistics

We conduct geographic information system (GIS) modeling to estimate the energy use and GHG emissions associated with the supply chain of the PEV batteries during their second life stage. We use geospatial optimization methods to identify the effects of supply chain logistics, integrating energy and environmental metrics [30]. A location-allocation analysis is used to determine the optimal facility locations, where the objective function minimizes the total weighted distance (ton-km) that the batteries must travel from their initial collection points to their second life locations and finally to the recycling facility. For modeling the supply chain logistics, the weighted distance is the appropriate function to

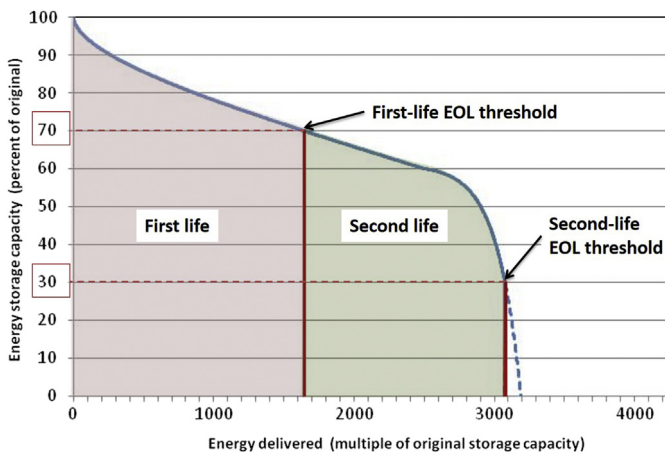


Fig. 3. Relation between first life and second life of batteries, as determined by the degradation profile and by the end-of-life thresholds of first and second lives (base-case is shown here).

minimize, as the environmental impacts are linearly related to the total distance traveled.

We model three alternative logistics scenarios for battery second-life use: decentralized solar, decentralized wind, and centralized wind/solar. The centralized scenario assumes that all batteries are used in a single large facility in Kern County, where the average solar and wind intensities are both greatest in California. The decentralized solar and wind scenarios assume that second-life batteries are distributed to different counties in proportion to each county's solar and wind (respectively) resources above a minimum threshold of viability. These three scenarios cover a range of potential battery distribution alternatives that may occur through 2050.

To quantify the impacts of transportation between battery collection points, dismantling facilities, second life locations, and recycling facilities, we assume batteries are transported via diesel truck. We create a network dataset in an ArcGIS software environment to calculate the transportation distances, using data on California's highway network and county borders sourced from the US Department of Commerce and the US Census Bureau [31]. Solar and wind intensity data are sourced from the US National Renewable Energy Laboratory [32]. Geographically-explicit car dealership locations are taken from Data Lists [33].

We assume battery packs are collected at local car dealerships, as these locations are currently used for battery testing and take-back [34]. The mass of batteries collected at each dealership is calculated based on the projected number, mass, and capacity of batteries disposed per county in 2050 (see Section 2.2). The transportation between consumers' homes and collection points is typically not accounted for in the literature, and is excluded from this model [35]. From the initial collection points, the batteries are transported to dismantling facilities for processing, where 10% of the battery mass is assumed to be diverted to traditional recycling [36]. The batteries are then transported to the location of their second-life applications, and at the end of their second life they are sent to a centralized battery recycling facility. For the facility location optimization, all California county centroids are considered as candidate locations [37]. GIS modeling provides the optimal facility locations for each logistics scenarios, and transportation energy use and GHG emissions are calculated. Fig. S3 shows the corresponding optimal facility locations for each scenario.

3. Results and discussion

Modeled results for PEV battery disposal in California through 2050, based on scenario projections of PEV adoption and first-life duration, are shown in Fig. 4. Under base-case conditions, about

60,000 metric tons of batteries per year are anticipated for 2050, ranging from 30,000 to 90,000 tons per year in the low and high scenarios. This battery supply represents about 15,000 MWh of original (at the time of purchase) energy storage capacity, ranging from 8000 to 25,000 MWh.

The energy use and GHG emissions of transporting batteries to and from their locations of second-life use are found to be relatively minor, based on results from the GIS analysis of supply-chain logistics. This includes collection of the batteries from dealerships, distribution of batteries to the second-life sites, and final transport from the second-life sites to a recycling facility. The centralized renewable scenario requires the least energy use (880 MJ of diesel fuel) and emits the least GHG (65.5 kg CO₂e), per ton of battery used in second-life applications. The decentralized wind scenario is medium intensity (1060 MJ ton⁻¹, and 78.8 kg CO₂e ton⁻¹). The decentralized solar scenario is most energy intensive (1240 MJ ton⁻¹) and GHG intensive (92.6 kg CO₂e ton⁻¹), and we use this as our base-case logistics scenario. Details on energy and GHG intensities of the 3 second-life logistics scenarios are listed in Table S5.

The energy balance under base-case conditions is shown in Fig. 5. In 2050, about 15 TWh of electricity are projected to be delivered by second-life PEV batteries. This will require about 18 TWh of renewable intermittent electricity for charging, taking into account the assumed round-trip efficiency of 80%. Cooling of the second-life batteries in use requires about 1 TWh of electricity. Energy use for transport of batteries to and from their locations of second-life use is comparatively minor.

The GHG balance under base-case conditions is shown in Fig. 6. In 2050, charging the second-life batteries will emit about 0.5 Mt CO₂e per year, due to life-cycle emissions from intermittent PV electricity generation. Discharging this electricity later during the diurnal cycle, to replace natural gas-fired electricity generation, will avoid about 7.5 Mt CO₂e per year. Battery transport and cooling are projected to cause relatively minor GHG emissions.

Fig. 7 shows the sensitivity to parameter variations of 3 performance metrics: cumulative electricity delivered, cumulative energy balance, and cumulative GHG reduction. The central axis of each figure shows the base case value of the metric, and each bar shows the effect of each individual parameter shifting to its low-performance value (left bars) and high-performance value (right bars). The metrics are all sensitive to the battery supply scenario, which directly affects the scale of second-life potential, and depends heavily on PEV adoption rates. These metrics are also sensitive to the battery degradation inflection point, when the batteries change from initial Phase 1 degradation to terminal Phase 2 degradation. The cumulative GHG reduction is sensitive to the

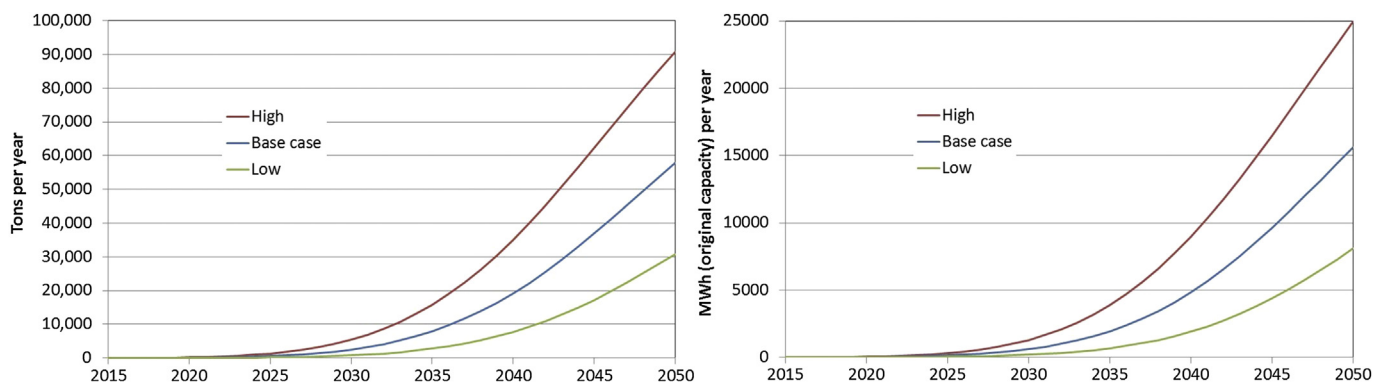


Fig. 4. Projected supply of disposed PEV batteries in California. Left figure shows tons of batteries disposed per year; right figure shows MWh of original storage capacity of batteries disposed each year.

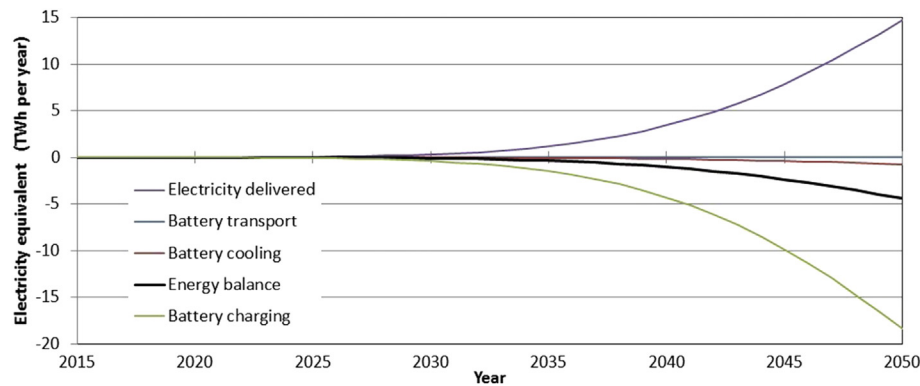


Fig. 5. Energy balance of modeled second-life battery use in California. Second-life batteries have the potential to deliver about 15 TWh of electricity per year in 2050.

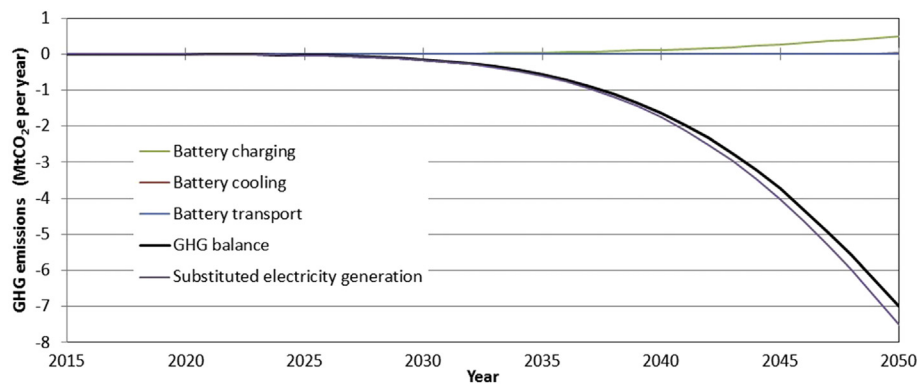


Fig. 6. GHG balance of modeled second-life battery use in California, assuming battery charging with distributed solar PV electricity, and battery discharging to displace natural gas-fired electricity generation. Potential net emissions reduction of about 7 Mt CO₂e per year is projected for 2050.

source of substituted electricity. If coal-fired electricity is displaced by the renewable intermittent electricity supported by second-life batteries (instead of base-case natural gas-fired electricity), the cumulative GHG emission reduction is doubled. This suggests that the overall climate benefits of second-life use of California's retired PEV batteries may be greater if the second-life application is outside of California, where coal-fired electricity is more common.

The ESOI performance of second-life systems is primarily affected by round-trip efficiency and cooling system COP. For base-case conditions, the $ESOI'$ metric of second-life battery use is 20. The broader $ESOI''$ metric, including energy investment for battery transportation and cooling as well as round-trip losses, is 4 under base-case conditions. The sensitivity of these performance metrics to parameter variations is shown in Fig. 8. The $ESOI_{B\&B}$ (see Equation (3)) of new lithium-ion batteries was estimated by Barnhart & Benson [15] at about 10, comparing the first-life electricity output to the primary energy investments for raw material supply and battery manufacture. The ESOI values calculated by Barnhart & Benson [15] are not to be directly compared with the ESOI metrics calculated here, as they measure fundamentally different phenomena. We present them here to encourage discussion on appropriate performance metrics for large-scale energy storage systems.

4. Conclusions

This exploratory analysis suggests that second-life use of retired PEV batteries may play a modest, though not insignificant, role in California's future energy system. The electricity delivered under base-case modeling conditions, 15 TWh per year in 2050 (Fig. 5 and

Table S6), is roughly 5% of the current total electricity use in California of about 300 TWh per year. The total anticipated electricity use in California in 2050 remains about 300 TWh per year, based on Scenario 2 of Greenblatt [38] which considers the effects of committed and uncommitted energy and climate policies through 2050. Electricity production from onshore wind, distributed PV, and centralized PV is anticipated to increase from current low values to about 100 TWh per year by 2050. The second-life battery use analyzed here is projected to support and enable part of this increased production, by storing electricity produced during peak generation periods and delivering it later during peak demand periods.

Under base-case modeling conditions, second-life battery use in California has the potential to reduce GHG emissions by about 7 Mt CO₂e per year in 2050 (Fig. 6 and Table S6). This is roughly 1.5% of current total California GHG emissions of 460 Mt CO₂e per year. It is about 4% of the anticipated total emission reduction from 2010 to 2050 of 150 Mt CO₂e per year (based on Scenario 2 of Greenblatt [38]). Emissions from producing electricity used in California are currently about 100 Mt CO₂e per year, and are anticipated to be about half that amount in 2050. The 7 Mt CO₂e per year avoided due to projected second-life battery use would comprise about 14% of that reduction in the electricity sector.

The magnitude of energy and climate benefits of second-life battery use is directly proportional to the number of retired vehicle batteries available, which depends strongly on the future adoption rate of PEVs in California. The PEV adoption rate, bounded by the slow and fast rates shown in Fig. 4, thus becomes a key uncertainty surrounding future benefits of second-life battery use in California. The capacity threshold for retirement of batteries

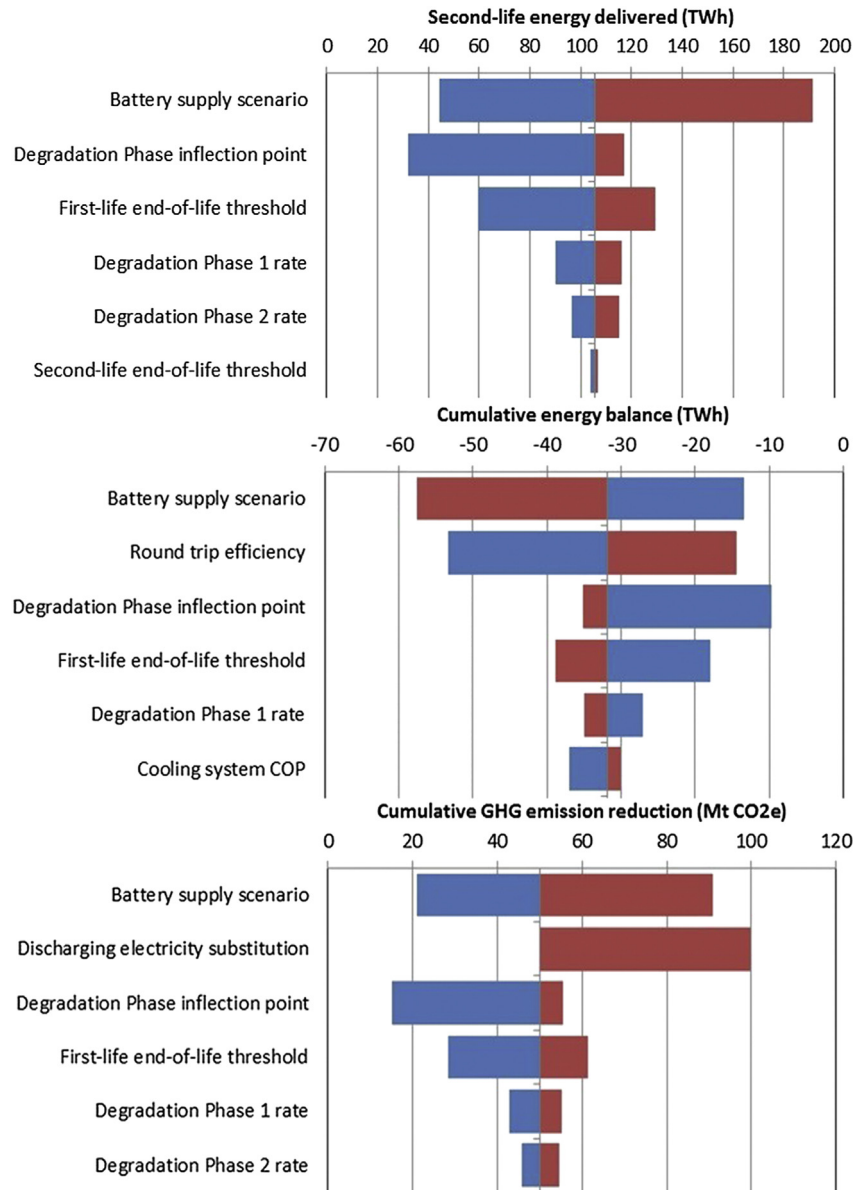


Fig. 7. Change in 3 metrics (cumulative, 2015–2050) due to variation of individual parameters between low and high values. From top to bottom: cumulative second-life electrical energy delivered; cumulative electrical energy balance; cumulative GHG emission reduction. For each metric, the six most significant parameters are shown.

from PEVs is also identified as an important variable. In our analysis the base-case threshold between first and second lives is 70% of original capacity, and moving this threshold to 60% or 80% is found to have a significant impact on second-life performance. PEV batteries are typically considered to be still useful in vehicles until they degrade to about 70% of their original capacity, though there has been little rational analysis to support this retirement threshold. Recent work suggests that PEV functionality remains high, even as the battery capacity drops below the commonly accepted threshold of 70% capacity. Saxena et al. [39] found that a large fraction of the mobility needs of US drivers continue to be satisfied with PEV batteries with less than 70% remaining capacity. This suggests that future rationalization of the retirement threshold may lengthen first lives of PEV batteries, and correspondingly shorten their second-life potential.

For any given amount of batteries produced, the degradation profile determines how much electricity can be stored and delivered by the batteries during their life spans. Acknowledging the

complexity of physical and chemical factors determining battery degradation, here we simply characterize the degradation based on three parameters: Phase 1 initial degradation rate, Phase inflection point between Phases 1 and 2, and Phase 2 terminal degradation rate. We find that the inflection point location has the greatest influence on second-life battery performance. Our base-case assumes that Phase 1 degradation continues until the battery reaches 60% of its original storage capacity, when terminal Phase 2 degradation begins. Delaying this inflection to 40% of original capacity significantly increases second-life opportunities, while early inflection at 80% of original capacity substantially decreases them. The rate of Phase 1 degradation has moderate impact on second-life, while the rate of Phase 2 degradation has very little impact. These results suggest that designing and building batteries such that terminal degradation is delayed or avoided, will enable much greater opportunities for second-life benefits.

The uncertainties of this analysis are substantial, due to the limited quantitative data available on performance of batteries

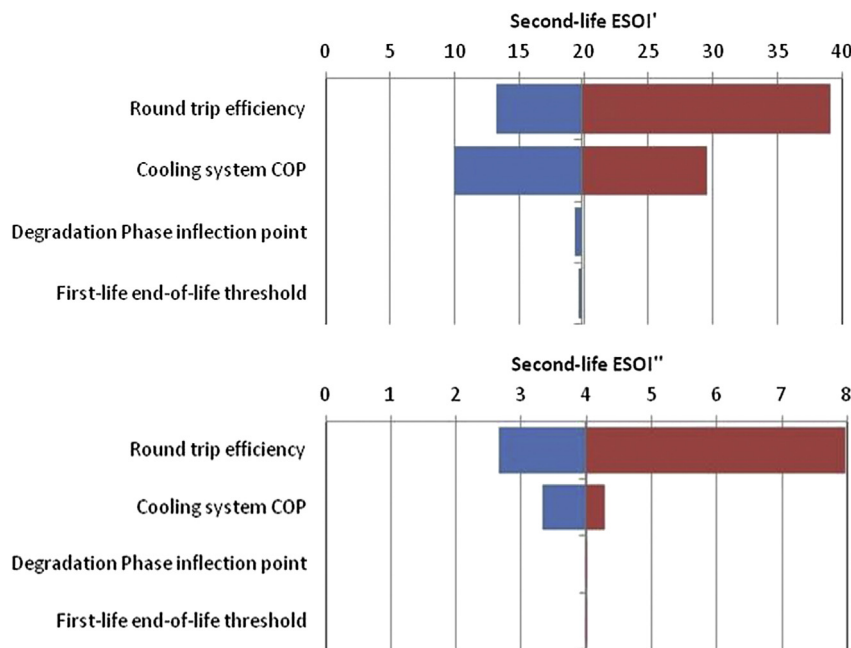


Fig. 8. Change in ESOI metrics due to variation of individual parameters between low and high values. Top figure shows $ESOI'$ including operational energy investments for battery transport and cooling. Bottom figure shows $ESOI''$ also including round-trip charge–discharge losses as operational energy investment. For each metric, the four most significant parameters are shown.

during their full life-cycle. Much more is known about battery performance during their earlier stages of use and degradation, while comparatively little detail is available to inform robust modeling of later stages of battery use and degradation. We accommodate this uncertainty by conducting a comprehensive sensitivity analysis of model parameters, to determine which system-wide factors are most critical for successful second-life battery use. We find that several parameters are particularly significant: PEV adoption rates, inflection point between initial and terminal degradation, threshold between first- and second-life applications, round-trip charge/discharge efficiency, and the source of electricity generation that is offset by enabled renewable generation. Future work should focus on understanding and optimizing these factors, to allow second-life PEV batteries to play a beneficial role in California's energy future.

Acknowledgments

We would like to thank Jeffery Greenblatt, Venkat Srinivasan, Samveg Saxena, Mark Caffarey, Brad Smith, and Dirk Spiers for their advice and guidance. The Lawrence Berkeley National Laboratory (LBNL) is a national laboratory of the US Department of Energy (DOE) managed by the University of California for the DOE under Contract Number DE-AC-02-05CH11231. This report was prepared as an account of work sponsored by the California Energy Commission (CEC) and pursuant to an M&O Contract with the DOE. Neither LBNL, DOE, CEC, nor any of their employees, contractors, or subcontractors, makes any warranty, express or implied, or assumes any legal liability or responsibility for the accuracy, completeness, or usefulness of any information, apparatus, product, or process disclosed, or represents that its use would not infringe on privately owned rights. The views and opinions of authors expressed herein do not necessarily state or reflect those of LBNL, DOE, CEC, or any of their employees, or the Government, or any agency thereof, or the State of California. This report has not been approved or disapproved by LBNL, the DOE, or the CEC, nor has

LBNL, the DOE, or the Sponsor passed upon the accuracy or adequacy of the information in this report.

Appendix A. Supplementary data

Supplementary data related to this article can be found at <http://dx.doi.org/10.1016/j.jpowsour.2015.04.097>.

References

- [1] SAFE (Securing America's Future Energy), Electric Vehicles: August 2014 Market Snapshot, 2014. <http://energypolicyinfo.com/2014/09/electric-vehicles-august-2014-market-snapshot/> (accessed 14.10.14.).
- [2] US National Academy of Sciences, Transitions to Alternative Vehicles and Fuels, The National Academies Press, Washington DC, 2013. http://www.nap.edu/catalog.php?record_id=18264 (accessed 14.09.14.).
- [3] University of California-Davis, PEV Market Briefing: May 2014, 2014. <http://policyinstitute.ucdavis.edu/files/PEV-Market-Briefing-Turrentine-28May2014.pdf> (accessed 7.05.14.).
- [4] T. Hendrickson, O. Kavvada, N. Shah, R. Sathre, C. Scown, Life-cycle implications and supply chain logistics of electric vehicle battery recycling in California, *Environ. Res. Lett.* 10 (2015) 014011.
- [5] B. Dunn, H. Kamath, J.M. Tarascon, Electrical energy storage for the grid: A battery of choices, *Science* 334 (2011) 928–935.
- [6] E. Cready, J. Lippert, J. Pihl, I. Weinstock, P. Symons, R.G. Jungst, Technical and economic feasibility of applying used EV batteries in stationary applications, Sandia Natl. Lab. (2003). Report SAND2002–4084.
- [7] C.K. Narula, R. Martinez, O. Onar, M.R. Starke, G. Andrews, Economic analysis of deploying used batteries in power systems, Oak Ridge Natl. Lab. (2011). Report ORNL/TM-2011/151.
- [8] J. Neubauer, A. Pesaran, The ability of battery second use strategies to impact plug-in electric vehicle prices and serve utility energy storage applications, *J. Power Sources* 196 (2011) 10351–10358.
- [9] B. Williams, T. Lipman, Analysis of the Combined Vehicle- and Post-Vehicle-Use Value of Lithium-Ion Plug-In-Hybrid Propulsion Batteries, Calif. Energy Comm. (2012). Report CEC-500-2013-088.
- [10] J.S. Neubauer, A. Pesaran, B. Williams, M. Ferry, J. Eyer, A Techno-economic Analysis of PEV Battery Second Use: Repurposed-battery Selling Price and Commercial and Industrial End-user Value, SAE Technical Paper No. 2012-01-0349, 2012.
- [11] H. Ambrose, D. Gershenson, A. Gershenson, D. Kammen, Driving rural energy access: A second-life application for electric-vehicle batteries, *Environ. Res. Lett.* 9 (2014) 094004.
- [12] L. Ahmadi, A. Yip, M. Fowler, S.B. Young, R.A. Fraser, Environmental feasibility of re-use of electric vehicle batteries, *Sustain. Energy Technol. Assess.* 6 (2014)

- 64–74.
- [13] R. Faria, P. Marques, R. Garcia, P. Moura, F. Freire, J. Delgado, A.T. de Almeida, Primary and secondary use of electric mobility batteries from a life cycle perspective, *J. Power Sources* 262 (2014) 169–177.
 - [14] T. Yuksel, J.J. Michalek, Effects of regional temperature on electric vehicle efficiency, range, and emissions in the United States, *Environ. Sci. Technol.* 49 (2015) 3974–3980.
 - [15] C.J. Barnhart, S.M. Benson, On the importance of reducing the energetic and material demands of electrical energy storage, *Energy & Environ. Sci.* 6 (2013) 1083–1092.
 - [16] C.D. Scown, M. Taptich, A. Horvath, T.E. McKone, W.W. Nazaroff, Achieving deep cuts in the carbon intensity of US automobile transportation by 2050: complementary roles for electricity and biofuels, *Environ. Sci. Technol.* 47 (2013) 9044–9052.
 - [17] US Energy Information Administration, Annual Energy Outlook 2013, DOE/EIA-0383(2013), US Energy Information Administration, Washington DC, 2013.
 - [18] A. Bandivadekar, K. Bodek, L. Cheah, C. Evans, T. Groode, J. Heywood, E. Kasseris, M. Kromer, M. Weiss, On the Road to 2035: Reducing Transportation's Petroleum Consumption and GHG Emissions, LFEE 2008-05 RP, MIT Laboratory for Energy and the Environment, Cambridge MA, 2008.
 - [19] A. Millner, Modeling lithium ion battery degradation in electric vehicles, in: IEEE Conference on Innovative Technologies for an Efficient and Reliable Electricity Supply (CITRES), 2010. <http://dx.doi.org/10.1109/citres.2010.5619782>.
 - [20] A. Barré, B. Deguilhem, S. Grolleau, M. Gérard, F. Suard, D. Riu, A review on lithium-ion battery aging mechanisms and estimations for automotive applications, *J. Power Sources* 241 (2013) 680–689.
 - [21] R. Spotnitz, Simulation of capacity fade in lithium-ion batteries, *J. Power Sources* 113 (2003) 72–80.
 - [22] J. Wang, P. Liu, J. Hicks-Garner, E. Sherman, S. Soukiazian, M. Verbrugge, H. Tataria, J. Musser, P. Finamore, Cycle-life model for graphite-LiFePO₄ cells, *J. Power Sources* 196 (2011) 3942–3948.
 - [23] S.L. Dolan, G.A. Heath, Life cycle greenhouse gas emissions of utility-scale wind: systematic review and harmonization, *J. Ind. Ecol.* 16 (2012) S136–S154.
 - [24] D.D. Hsu, P. O'Donoghue, V. Fthenakis, G.A. Heath, H.C. Kim, P. Sawyer, J.K. Choi, D.E. Turney, Life cycle greenhouse gas emissions of crystalline silicon photovoltaic electricity generation: systematic review and harmonization, *J. Ind. Ecol.* 16 (2012) S122–S135.
 - [25] H.C. Kim, V. Fthenakis, J.K. Choi, D.E. Turney, Life cycle greenhouse gas emissions of thin-film photovoltaic electricity generation: systematic review and harmonization, *J. Ind. Ecol.* 16 (2012) S110–S121.
 - [26] P. O'Donoghue, G.A. Heath, S.L. Dolan, M. Vorum, Life cycle greenhouse gas emissions of electricity generated from conventionally produced natural gas: systematic review and harmonization, *J. Ind. Ecol.* 18 (2014) 125–144.
 - [27] M. Whitaker, G.A. Heath, P. O'Donoghue, M. Vorum, Life cycle greenhouse gas emissions of coal-fired electricity generation: systematic review and harmonization, *J. Ind. Ecol.* 16 (2012) S53–S72.
 - [28] A. Hamidi, L. Weber, A. Nasiri, EV charging station integrating renewable energy and second-life battery, in: International Conference on Renewable Energy Research and Applications (ICRERA), 2013.
 - [29] S. Tong, M. Klein, Second Life Battery Pack as Stationary Energy Storage for Smart Grid, SAE Technical Paper No. 2014-01-0342, 2014.
 - [30] J.J. Corbett, J.S. Hawker, J.J. Winebrake, Development of a California Geospatial Intermodal Freight Transport Model with Cargo Flow Analysis, California Air Resources Board, Sacramento, CA, 2010. <http://www.arb.ca.gov/research/apr/past/07-314.pdf> (accessed 10.11.13.).
 - [31] US Census Bureau, TIGER (Topologically Integrated Geographic Encoding and Referencing) Products. <https://www.census.gov/geo/maps-data/data/tiger.html> (accessed 20.11.13.).
 - [32] National Renewable Energy Laboratory, Dynamic Maps, GIS Data, and Analysis Tools. <http://www.nrel.gov/gis/maps.html> (accessed 20.10.14.).
 - [33] Data Lists, New Car Dealership Database, Data Lists, Omaha NE. <http://www.data-lists.com/new-car-dealership-database/> (accessed 2.02.14.).
 - [34] B. Smith, Personal Communication, Nissan North America, Houston TX, 2014.
 - [35] A.G. Yeh, M.H. Chow, An integrated GIS and location-allocation approach to public facilities planning: an example of open space planning, *Comput. Environ. Urban Syst.* 20 (1996) 339–350.
 - [36] D. Spiers, Personal Communication, ATC New Technologies, Oklahoma City OK, 2014.
 - [37] M. Vidovic, B. Dimitrijevic, B. Ratkovic, V. Simic, A novel covering approach to positioning ELV collection points, *Resour. Conserv. Recycl.* 57 (2011) 1–9.
 - [38] J.B. Greenblatt, Modeling California policy impacts on greenhouse gas emissions, *Energy Policy* 78 (2015) 158–172.
 - [39] S. Saxena, C. Le Floch, J. MacDonald, S. Moura, Quantifying EV battery end-of-life through analysis of travel needs with vehicle powertrain models, *J. Power Sources* 282 (2015) 265–276.